

ORIGINAL ARTICLE

LRFN2 binding to NMDAR inhibits the progress of ESCC via regulating the Wnt/ β -Catenin and NF- κ B signaling pathway

Yu Zhou¹  | Lijuan Xu¹ | Jiru Wang¹ | Beibei Ge¹ | Qiuzi Wang¹ | Tao Wang¹ | Chang Liu¹ | Bin Wei¹ | Qilong Wang²  | Yong Gao¹ 

¹Department of Medical Oncology, Cancer Center, The Affiliated Huaian No. 1 People's Hospital of Nanjing Medical University, Huai'an, China

²Department of Central Laboratory, Cancer Center, The Affiliated Huaian No. 1 People's Hospital of Nanjing Medical University, Huai'an, China

Correspondence

Yong Gao, Department of Medical Oncology, Cancer Center, The Affiliated Huaian No. 1 People's Hospital of Nanjing Medical University, Huai'an 223300, China.

Email: hayygaoy@njmu.edu.cn

Qilong Wang, Department of Central Laboratory, Cancer Center, The Affiliated Huaian No. 1 People's Hospital of Nanjing Medical University, Huai'an 223300, China.

Email: qlwang@njmu.edu.cn

Funding information

Natural Science Foundation of Jiangsu Province, Grant/Award Number: BK20211111 and BK20211112; Nanjing Medical University, Grant/Award Number: NMUB2020133

Abstract

As a neuronal transmembrane protein, leucine-rich repeat and fibronectin type-III domain-containing protein 2 (LRFN2) can recruit and combine with *N*-methyl-D-aspartate receptors (NMDARs) to promote nerve growth. Genetic studies suggest that mutations in LRFN2 are associated with various cancers. However, the role and mechanism of LRFN2 in the progression of ESCC have not been elucidated. In this study, we demonstrated that LRFN2 was significantly downregulated in ESCC tissues by qRT-PCR and immunohistochemistry. Low LRFN2 expression was an adverse prognostic factor in patients with ESCC. Overexpression of LRFN2 effectively suppressed the proliferation, migration, invasion, and epithelial-to-mesenchymal transition in vitro and tumor growth in vivo. Bioinformatics analysis indicated that Wnt/ β -catenin signaling regulation was one of the most potential mechanisms and studies confirmed that overexpression of LRFN2 obviously downregulated the expression of β -catenin, c-Myc, and cyclin D1 in ESCC cells and tumor tissues. Further studies revealed that LRFN2 plays an anti-ESCC role by binding with NMDAR-GRIN2B and this effect can be weakened by NR2B-selective NMDA antagonist-NMDA-IN-1. Moreover, the bioinformatics analysis showed that the interaction of GRIN2B and GSK3 β affects the NF- κ B pathway, which was demonstrated by western blot experiments. Collectively, our results indicate that LRFN2 binding to NMDARs inhibits the progression of ESCC by regulating the Wnt/ β -catenin and NF- κ B pathway, which provides a new therapeutic target for improving the prognosis of patients with ESCC.

KEYWORDS

esophageal squamous cell carcinoma, LRFN2, NMDAR, Wnt/ β -catenin signaling pathway, NF- κ B signaling pathway

Abbreviations: EMT, epithelial-mesenchymal transition; ESCC, esophageal squamous cell carcinoma; GRIN2B, NMDA receptor 2B subunit; LRFN2, leucine-rich repeat and fibronectin type-III domain-containing protein 2; NMDAR, *N*-methyl-D-aspartate receptor; qRT-PCR, quantitative RT-PCR; TCGA, The Cancer Genome Atlas.

Yu Zhou and Lijuan Xu contributed equally to this work.

This is an open access article under the terms of the [Creative Commons Attribution-NonCommercial-NoDerivs](https://creativecommons.org/licenses/by-nc-nd/4.0/) License, which permits use and distribution in any medium, provided the original work is properly cited, the use is non-commercial and no modifications or adaptations are made.

© 2022 The Authors. *Cancer Science* published by John Wiley & Sons Australia, Ltd on behalf of Japanese Cancer Association.

1 | INTRODUCTION

Esophageal carcinoma is the seventh most commonly diagnosed cancer globally and sixth leading cause of cancer-related mortality based on GLOBOCAN 2020.¹ ESCC is the predominant histological type of esophageal carcinoma, representing more than 90% of esophageal cancers in Asia.² At present, few predictive factors exist for ESCC prognosis, except cancer staging, which is required for adjuvant treatment. Despite recent advances in chemoradiotherapy modalities, the survival rates of patients with ESCC remain poor, with a 5-year survival rate of 15%–25% after initial diagnosis.^{2–4} Although multiple gene mutations, including those in TP53, CDKN2A, PIK3CA, and NOTCH1, have been extensively reported in ESCC,^{5–7} their key roles in molecular pathogenesis are largely unknown. Therefore, identifying novel and effective prognostic factors and therapeutic targets for ESCC remains an urgent unmet medical need.

As a neuronal transmembrane protein, leucine-rich repeat and fibronectin type-III domain-containing protein 2 (LRFN2) can recruit and combine with *N*-methyl-D-aspartate receptor (NMDARs) through the C-terminal PDZ domain to promote neurodevelopment.^{8–10} Interestingly, genetic studies suggest that mutations in LRFN2 are associated with various cancers.^{11–13} In a genome-wide association study, single nucleotide polymorphisms in strong linkage disequilibrium (LD) with rs2494938 at 6p21.1 are located in the initial region (including promoter, exon 1, and intron 1) of LRFN2, which has been proven to be tumor specific in the susceptibility to multiple cancers, including ESCC.¹¹ Moreover, our previous research demonstrated that this LRFN2 polymorphism emerged as an independent prognostic marker of ESCC in the Chinese population.¹³ In this study, LRFN2 was shown to be a cancer suppressor with abnormally low expression in cancer tissues and was correlated with the prognosis of ESCC. This suggests that LRFN2 may play a vital role in the occurrence and progression of ESCC.

NMDARs are excitatory neurotransmitter receptors of the central nervous system,¹⁴ and functional NMDARs usually play a role in the formation of ion channels regulated by glutamate and glycine.¹⁵ In neurons, NMDAR family members exhibit different tissue distributions, expression patterns, and functions. Aberrant expression of NMDARs also occurs in many cancers and is linked to the initiation, progression, and poor prognosis of multiple types of tumors. While active NMDARs have an important influence on the growth and survival of some cancers,^{16,17} NMDAR2B is epigenetically inactivated and exhibits tumor-suppressive activity in ESCC because its promoter methylation commonly exists in the tumor to abrogate gene transcription, thereby leading to cellular resistance to apoptosis.^{18,19} Therefore, both LRFN2 and NMDAR2B possess tumor-suppressive activity in ESCC. Although LRFN2 can bind to the NMDAR subunit through its extracellular or transmembrane domains,^{8,20} whether LRFN2 exerts antitumor effects through NMDARs and the role and mechanism of the LRFN2/NMDAR complex in ESCC have not been elucidated.

In this study, we provide evidence that elevated expression of LRFN2 regulates the Wnt/ β -catenin pathway and NF- κ B pathway by binding to NMDAR, thereby suppressing tumor progression.

Novelty and impact

Our study is the first to show that leucine-rich repeat and fibronectin type-III domain-containing protein 2 (LRFN2) can bind to the *N*-methyl-D-aspartate receptor (NMDAR) to inhibit the Wnt/ β -catenin pathway and the NF- κ B pathway. Our findings support the utility of LRFN2 as a potential therapeutic target for inhibiting the development of esophageal cancer and a useful independent prognostic marker of patient survival.

2 | MATERIAL AND METHODS

2.1 | Sources of ESCC patients and collection of tissue specimens

We collected tumor tissue and paired normal esophageal epithelial tissue from 67 patients with ESCC who underwent radical surgery and did not receive preoperative radiotherapy or chemotherapy at the Esophageal Cancer Specimen Bank of Affiliated Huai'an No. 1 People's Hospital of Nanjing Medical University (Huai'an, China). None of the patients received radiotherapy or chemotherapy before surgery. All the cases were staged according to the TNM staging system of the American Joint Committee on Cancer (AJCC 7th edition, 2010), histologically diagnosed independently by two experienced pathologists. After radical resection of esophageal cancer, tumor tissue and paracancer tissue specimens were preserved with liquid nitrogen for subsequent experiments. This study was approved by the Ethical Committee of Huai'an No. 1 People's Hospital, Nanjing Medical University (YX-P-2020-065-01), and informed consent of all patients was obtained before the study was conducted.

2.2 | ESCC cell lines and culture conditions

Two human ESCC cell lines (TE1 and KYSE30) were purchased from the Cell Bank of the Chinese Academy of Sciences (Shanghai, China). The cells were cultured in DMEM-high supplemented with 10% fetal bovine serum (Clark, AUS). All cell lines were maintained in a humidified incubator at 37°C in an atmosphere of 5% CO₂.

2.3 | ESCC cell transfection

LRFN2 silencing was achieved using small interfering RNA (siRNA). Transfection of siRNA was performed using Lipofectamine 2000 Reagent (Invitrogen, Carlsbad, USA). The LRFN2 siRNA (siLRFN2) sequence was 5'-GAGGAAAAGAGUGUCUUUU-3' and the negative control sequence was 5'-UUCUCCGAACGUGUCACGU-3' (General Biol, Anhui, China).

2.4 | Lentivirus production and cell transfection

According to the characteristics of the LRFN2 protein, the Chinese plasmid and protein shared library (PPL) was used to design and to synthesize a lentivirus vector with puromycin resistance and a negative control for LRFN2. Both vectors were transfected into the ESCC cell lines. At 48 h post-transfection, the cells were selected with puromycin (1 $\mu\text{g}/\text{ml}$) for 2 weeks to construct cell lines with stable LRFN2 overexpression. Transfection efficiency was verified using qRT-PCR.

2.5 | RNA extraction and quantitative RT-PCR

Total RNA was isolated from patient tissues and cultured cells using TRIzol reagent (Thermo, USA) according to the manufacturer's instructions and reverse transcribed using the FastQuant RT Kit (Tiangen, Beijing, China). The PCR was performed in triplicates with SuperReal PreMix Plus (Tiangen) using the Real-Time PCR Detection System (Roche, California, USA). The specific primers for LRFN2 were forward: 5'-TGGGCGGCAACTTCATCATC-3' and reverse: 5'-CAGCCGATTGCTGTCAAGA-3'. The forward and reverse primers for GAPDH were 5'-ACCAGCCTCAAGATCATCAGC-3' and 5'-TGCTAAGCAGTTGGTGGTGC-3', respectively. Each sample was run in triplicate and fold changes were calculated using the relative quantification $2^{-\Delta\Delta\text{CT}}$ method.

2.6 | Cell proliferation assay

TE1 and KYSE30 cells were inoculated into 96-well plates at a density of 2000 cells/100 μl , respectively, and CCK-8 (Dojindo, Japan) was added at different observation times. The parameters of the microplate reader (Bio Tek, Winooski, USA) were set to 450 nm, the plates were put into the machine according to the observation time, the absorbance was measured and recorded. The colony formation test was also one of the experimental methods we used to evaluate the proliferation ability of tumor cells. TE1 and KYSE30 were collected and suspended simultaneously to ensure that cells did not aggregate. In total, 200 cells were planted evenly on six-well plates, and the freshly configured medium was changed periodically. After 2 weeks of culture, the above two cell types were discarded and washed, fixed with paraformaldehyde, and stained with crystal violet according to the standard protocol. Cells can be seen forming colonies, the number of colonies was counted and recorded. The experiment was repeated three times, and the mean was calculated.

2.7 | Cell migration and invasion assays

Cell migration ability was measured using transwell chambers (8- μm pore size; Corning Costar, Cambridge, MA, USA). For the transwell assay, 50,000 cells/100 μl suspended in serum-free DMEM were

inoculated into the upper chamber. The lower chamber contained DMEM supplemented with 10% serum, which served as a chemoattractant. After 24 or 48 h of incubation, the filters were fixed in methanol and stained with 0.1% crystal violet. The upper faces of the filters were gently abraded, and the lower faces with cells migrating across the filters were imaged and counted under a microscope. Cell invasion ability was measured using transwell chambers mixed with Matrigel (8- μm pore size; Corning Costar, Cambridge, MA, USA). The transwell chambers were placed in a 24-well plate, and serum-free DMEM was mixed with Matrigel. Then, 100 μl of this mixture was added into the upper chamber and placed in a 37°C incubator until the gel solidified (4–6 h). The remaining steps were consistent with those of the migration assay. These experiments were performed in triplicate and repeated three times.

2.8 | Xenograft tumor model in nude mice

NOD/SCID male mice aged 4–5 weeks were purchased from Nanjing Medical University and raised in a specific pathogen-free (SPF) animal house. KYSE30 cells transfected with lentivirus or empty vector containing LRFN2 sequence were subcutaneously inoculated in the right axilla of the mice. The SPF animal room was accessed every day to observe the morphologic changes of the subcutaneous transplanted tumors and record them in detail. After continuous observation for 4 weeks, animals were sacrificed according to animal ethics requirements, xenograft tumors were dissected and weighed, and some tumor tissues were collected for immunohistochemical analysis, H&E staining, western blot, and other experiments. All experiments were approved by the Animal Care and Use Committee of The Affiliated Huaian No. 1 People's Hospital of Nanjing Medical University (DW-P-2018-007-01).

2.9 | Immunohistochemical analysis

The dissected tumors from the 67 patients were paraffin embedded and cut into 4- μm sections. The sections were deparaffinized and rehydrated. After antigen retrieval, the sections were incubated with anti-LRFN2 (Abcam, Cambridge, UK) and anti-GRIN2B (Abcam) antibodies at 4°C overnight. After incubation with horseradish peroxidase-conjugated secondary antibody (Dako, Glostrup, Denmark), the sections were counterstained with Mayer's hematoxylin. Mouse tumor sections were incubated with anti-LRFN2 and anti-Ki-67 antibodies (Abcam), and the remaining steps were as described previously. The immunostaining score was independently evaluated by two pathologists. Quantitative analysis was performed using image analysis software. The cumulative optical density (IOD) is the value obtained by adding up all the optical density values of each brown point on the image. The average optical density (mean density) is the value obtained by dividing the IOD by the area (area) of the effective target distribution area. Quantitative analysis was performed by comparing the average optical density between groups.

2.10 | Co-immunoprecipitation, western blot, and immunofluorescence staining

Cells were washed with phosphate-buffered saline (137mM NaCl, 2.7mM KCl, 10mM Na₂HPO₄, and 2mM KH₂PO₄) and ice-cold RIPA

lysis buffer (50mM Tris-HCl pH 7.4, 150mM NaCl, 1% NP-40, 1mM EDTA, 2mM PMSF, and protease inhibitor) was added. Cells were lysed for 30min at 4°C with occasional vortexing. The lysates were centrifuged for 10 min at 12000 g. The supernatants (whole cell extracts) were incubated with different antibodies and protein A/G

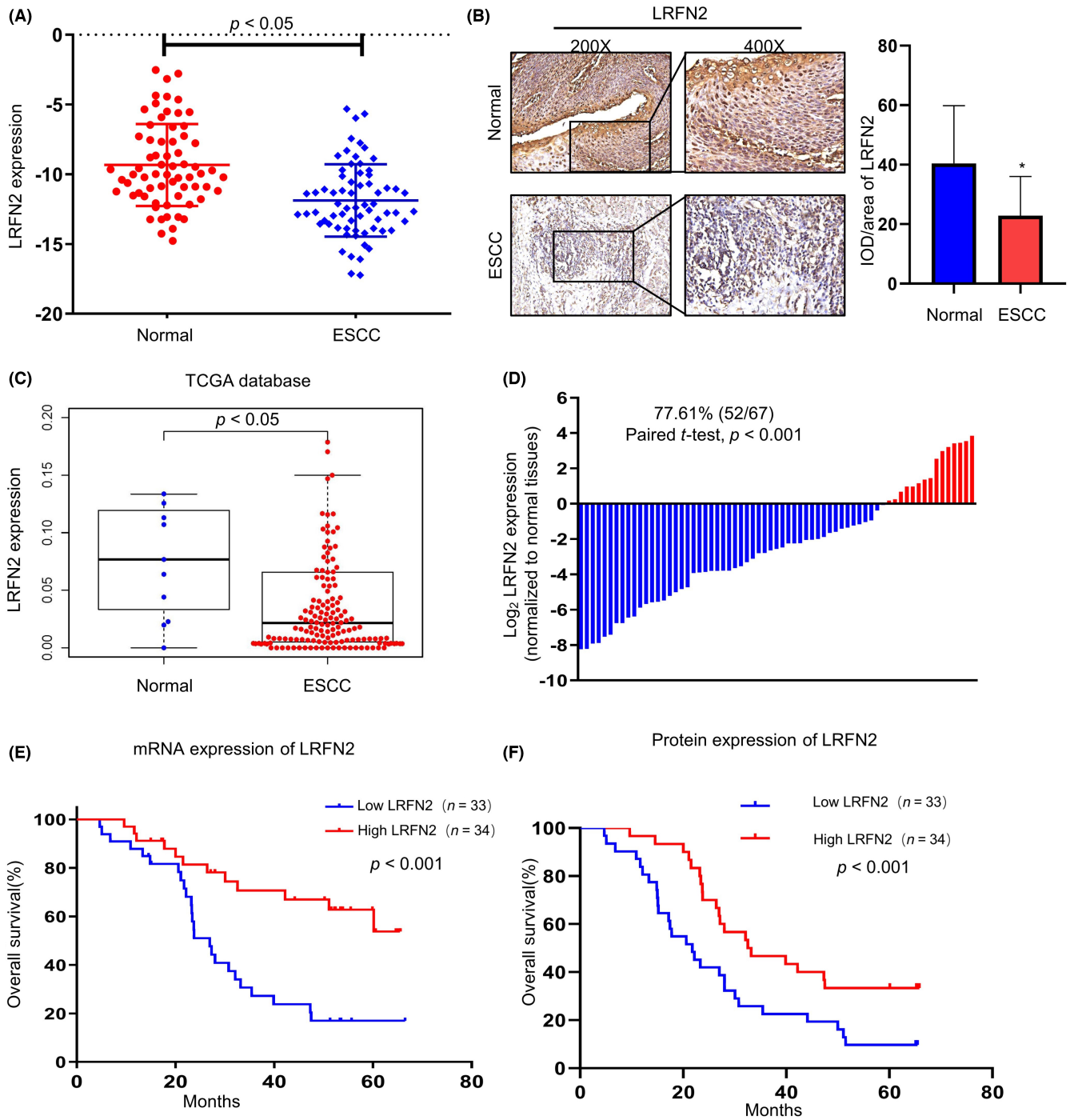


FIGURE 1 LRFN2 expression is decreased in esophageal cancer tissues. (A, B) Both the mRNA and protein expression of LRFN2 in ESCC tissues was markedly decreased compared with normal tissues. * $p < 0.05$. (C) In TCGA database, LRFN2 expression was decreased in squamous cell carcinoma tissues compared with normal tissues. (D) qPCR was used to detect LRFN2 mRNA expression in 67 ESCC tissues and adjacent nontumor tissues. (E) Based on the mRNA expression of LRFN2, 67 samples were divided into two groups: a high expression group ($n = 34$) and a low expression group ($n = 33$). Kaplan–Meier survival analysis showed that the high expression group had a better prognosis. (F) Based on the protein expression of LRFN2, 67 samples were divided into two groups: a high expression group ($n = 34$) and a low expression group ($n = 33$). Kaplan–Meier survival analysis showed that the high expression group had a better prognosis. * $p < 0.05$.

beads (Sigma-Aldrich) for 5 h at 4°C. The beads were washed five times with RIPA lysis buffer (20mM Tris-HCl pH 8.0, 100mM NaCl, 1mM EDTA, 0.5% NP-40, and 1mM PMSF). Bound proteins were extracted with SDS-PAGE sample buffer and analyzed by SDS-PAGE, followed by western blot analysis. For immunofluorescence staining, cells were seeded on glass coverslips in 24-well plates and grown overnight. The cells were then fixed in 4% paraformaldehyde for 20 min and permeabilized with 0.25% Triton X-100 for 10 min. After blocking with 4% bovine serum albumin for 1 h, the coverslips were incubated with primary antibody (4°C, overnight) such as anti-F-actin (Abcam), anti-LRFN2 (Abcam), anti-GRIN2B (Abcam), and anti-PSD-95 (Proteintech, China), followed by incubation with a fluorescent secondary antibody. Cell nuclei were stained using 4',6'-diamidino-2-phenylindole dihydrochloride (Life Technologies, Carlsbad, CA, USA). Images of the coverslips were observed using a confocal laser scanning microscope (FV1000; Olympus, Tokyo, Japan).

2.11 | Statistical analyses

For all comparisons, $p < 0.05$ was considered statistically significant. For categorical variables, we calculated proportions and 95% CIs. Number (%) for categorical variables. Values are presented as the mean \pm standard deviation for data that were normally distributed or median and interquartile range for data that were not normally distributed for continuous variables. For continuous variables, we calculated the median and interquartile range (IQR). Comparisons of distributions between two groups were made using the Mann-Whitney *U*-test, and pairwise comparisons were performed using Wilcoxon's signed rank test. The Mann-Whitney *U*-test was used for comparison between two groups. Nonparametric data with multiple comparisons were analyzed using Kruskal-Wallis one-way ANOVA followed by Holm's Stepdown Bonferroni procedure for adjusted *p*-values. Comparisons of distributions between three groups were made by Kruskal-Wallis test (including Dunn-Bonferroni post hoc correction). The Kolmogorov-Smirnov test was used to inspect the normality and homogeneity of variance of all the data. For two-group comparison, *p*-values were derived from the one-way Student's *t*-test to determine differences between groups with normally distributed data. Data with normal distribution were analyzed by ANOVA with Dunnett's post test or Tukey's correction for multiple comparisons. In the statistical calculation and analysis of the raw data, the software used was SPSS 26.0 (Chicago, Illinois, USA) and GraphPad Prism 8 (La Holla, California, USA).

3 | RESULTS

3.1 | Low expression of LRFN2 was associated with poor prognosis in ESCC patients

To assess whether LRFN2 played a crucial role in ESCC, the expression of LRFN2's mRNA and protein in 67 paired samples, including from both tumor and nontumor tissues that were removed from

the same patient during surgery, were determined and the results (Figure 1A,B, $*p < 0.05$) demonstrated that the expression of LRFN2 decreased more in tumor specimens than in nontumor specimens. The expression was further confirmed by analyzing The Cancer Genome Atlas (TCGA) database (Figure 1C).

To reveal the correlation between LRFN2 expression and clinical characteristics of ESCC patients, all ESCC patients were divided into a high expression group and a low expression group using median LRFN2 expression as the boundary (Figure 1D). Further analysis showed that LRFN2 expression was statistically correlated with TNM staging ($p = 0.008$; Table 1) and there was no significant correlation with age, sex, degree of differentiation, and tumor location (Table 1). Kaplan-Meier analysis showed that patients with low expression of LRFN2 in tumor tissues had significantly shorter overall survival than patients with high expression (Figure 1E,F). These data indicated that LRFN2 acts as an anti-oncogene and is closely related to ESCC development.

3.2 | LRFN2 inhibits proliferation, migration, and invasion of ESCC cells

The expression of LRFN2 was detected by western blot in various esophageal cancer cell lines, and the cell lines with relatively high and relatively low expression were screened (Figure S1). To verify the epigenetic function of LRFN2 in ESCC, LRFN2 overexpression cells were constructed by transfection pLVX-IRES-Puro-3xHA-LRFN2

TABLE 1 Relationship between LRFN2 mRNA expression and clinicopathological features of ESCC

Clinical features	Cases	LRFN2 expression		<i>p</i> -value
		Low	High	
Number, <i>n</i>	67	33	34	
Sex				
Male	45	22	23	0.932
Female	22	11	11	
Age, years				
≤ 65.5	33	17	16	0.751
> 65.5	34	16	18	
Tumor location				
Upper	5	3	2	0.500
Middle	49	22	27	
Under	13	8	5	
Differentiation				
G1	9	4	5	0.756
G2/G3	58	29	29	
TNM stage				
I	1	0	1	0.008
II	34	11	23	
III	32	22	10	

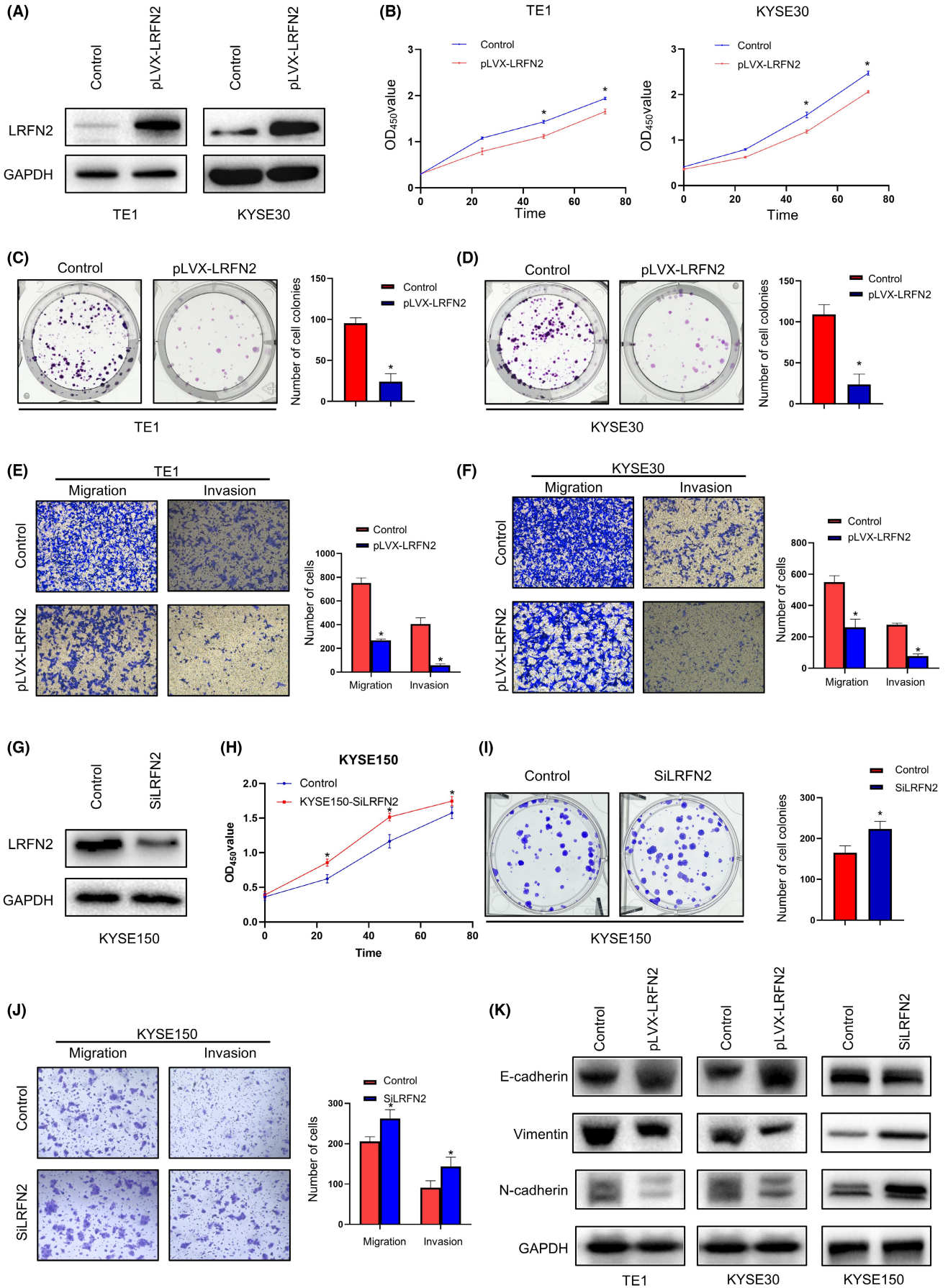


FIGURE 2 LRFN2 inhibits ESCC proliferation, invasion, and metastasis in vitro. (A) Infection of ESCC TE1 and KYSE30 cells with lentiviral vector pLVX-IRES-Puro-3xHA-LRFN2 (pLVX-LRFN2). The efficiency of LRFN2 overexpression in TE1 and KYSE30 cells was determined via western blot. (B) LRFN2 inhibited the proliferation of ESCC TE1 and KYSE30 cells. (C, D) The number of colonies formed by TE1 and KYSE30 overexpressing LRFN2 was reduced compared with the control group. (E, F) Effects of stable overexpression of LRFN2 on invasion and migration of TE1 and KYSE30 cells. The invasion and migration ability of ESCC cells was inhibited. (G) Knockdown of LRFN2 expression in KYSE30 using siRNA. The efficiency of LRFN2 low expression in KYSE150 cells was determined via western blot. (H) After downregulation of the expression of LRFN2, the growth rate of KYSE150 was faster than that of the control group. (I) The number of colonies formed by KYSE150 knockdown LRFN2 was reduced compared with the control group. (J) Knockdown of LRFN2 in KYSE150 cells produced an enhanced invasion and migration ability compared with the control group. (K) Western blotting was used to detect EMT-related protein levels. In TE1, KYSE30, and KYSE150 cells, overexpression of LRFN2 resulted in upregulation of E-cadherin expression, but downregulation of vimentin and N-cadherin expression. After knocking down LRFN2 expression, the opposite result was obtained. * $p < 0.05$.

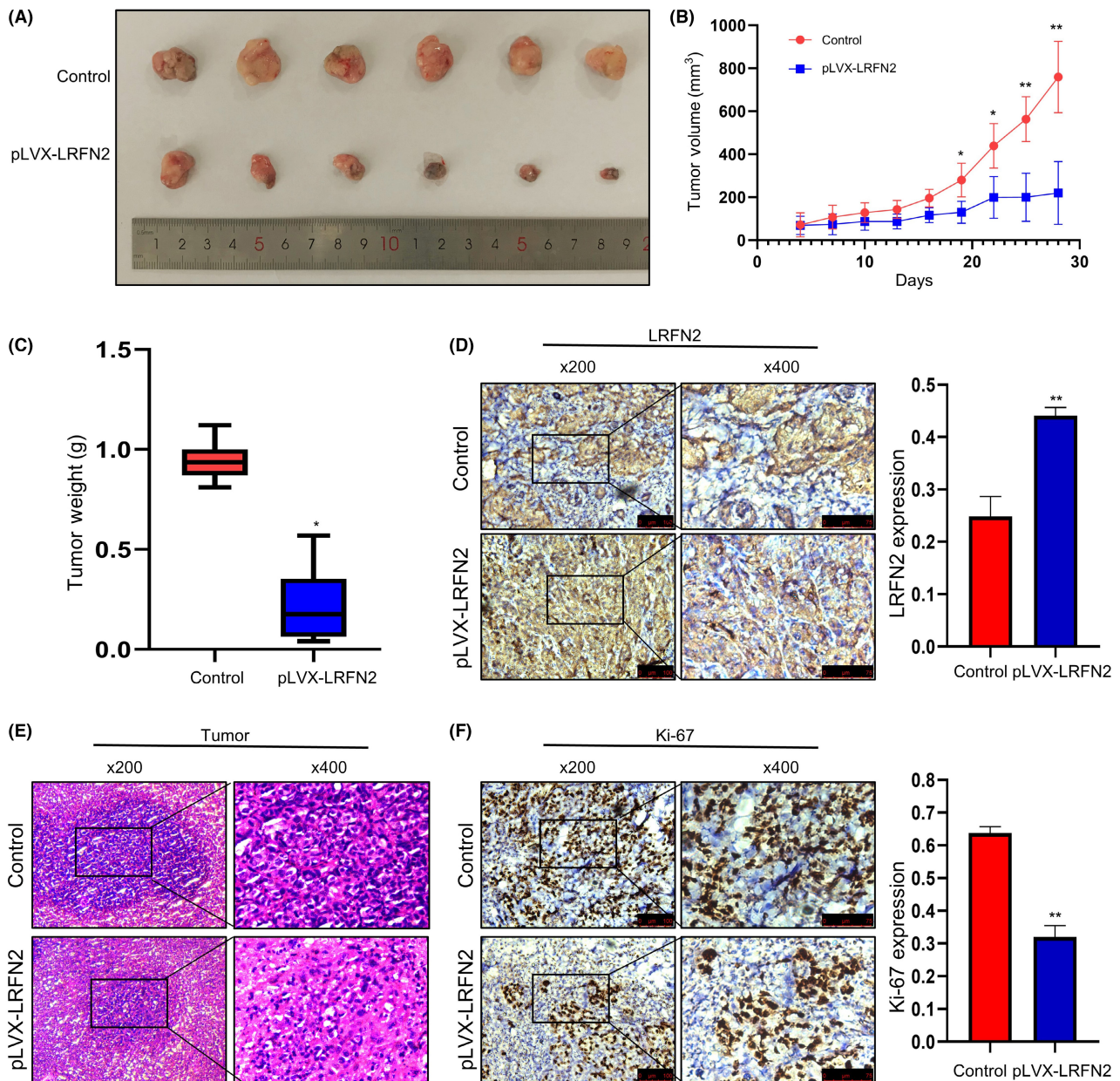


FIGURE 3 LRFN2 inhibits the growth of transplanted tumor in NOD/SCID mice. (A–C) In comparison with the control group, the size, tumor volume, and growth rate of subcutaneous tumor formation with KYSE30 cells overexpressing LRFN2 was significantly lower. (D) LRFN2 expression increased in the overexpression group, compared with the control group. (E) Pathology of the transplanted tumor in the two groups after H&E staining. In the control group, enlarged nuclei, deep staining, increased mitosis, and obvious tissue atypia were observed in the cancer cells, whereas the pLVX-LRFN2 group showed lighter staining, smaller nuclei, and less tissue atypia, indicating that LRFN2 can cause histomorphological changes in esophageal carcinoma. (F) Comparison of Ki67 in two groups of transplanted tumors. Expression of Ki67 was significantly decreased in the pLVX-LRFN2 group with LRFN2 overexpression. ** $p < 0.001$.

into ESCC cells such as TE1 and KYSE30 and the effect of virus vector transfection was verified by western blotting (Figure 2A). The results of cytological analyses demonstrated that the proliferation (Figure 2B–D, $*p < 0.05$), migration, and invasion (Figure 2E,F, $*p < 0.05$) of ESCC cells (TE1, KYSE30) were significantly suppressed by LRFN2 overexpression.

At the same time, we used siRNA to reduce the expression of LRFN2 in KYSE150 cells (Figures 2G and S2). We found that when the expression level of LRFN2 was decreased, the cells grew faster (Figure 2H,I; $*p < 0.05$), and their invasive and migratory abilities were enhanced (Figure 2J; $*p < 0.05$).

Further analysis revealed that the EMT-related protein E-cadherin was upregulated, the N-cadherin and vimentin were downregulated in LRFN2 overexpression cells, contrary to the knockdown group results (Figure 2K), indicating that LRFN2 may regulate the expression of key proteins in EMT-related pathways, therefore affecting the motor capacity of ESCC cells.

3.3 | LRFN2 inhibits the ESCC tumor growth in vivo

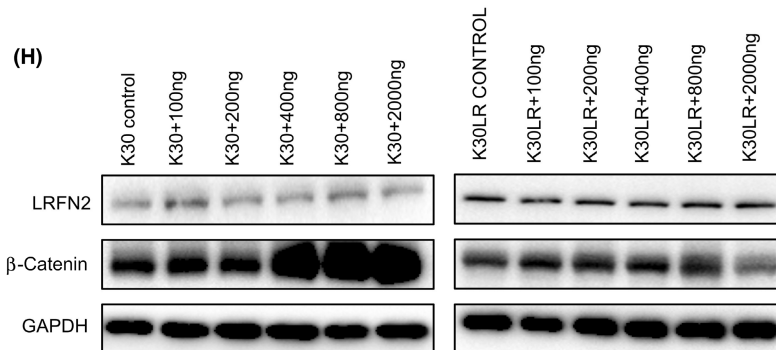
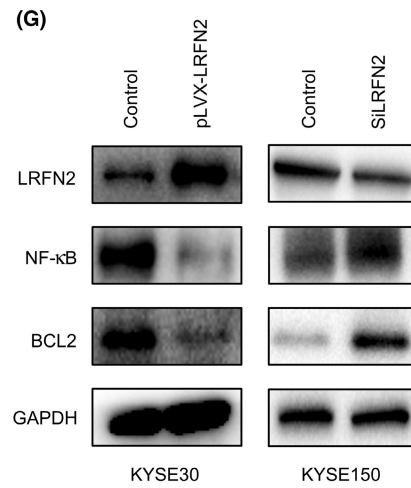
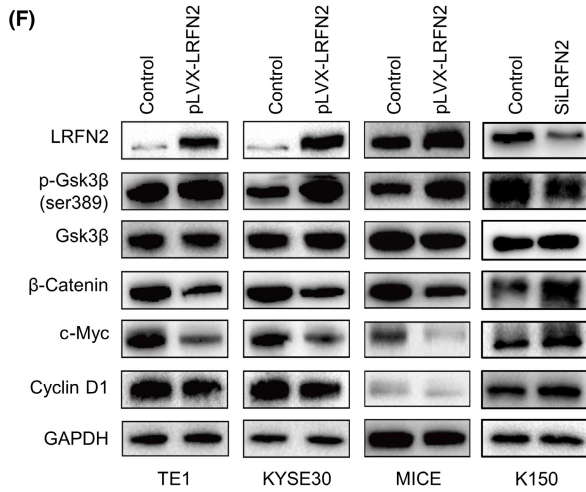
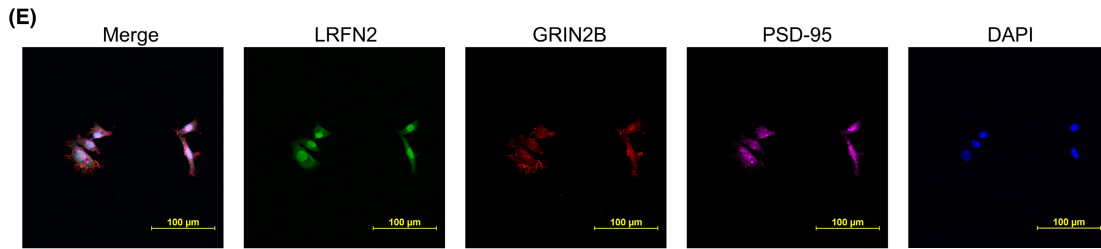
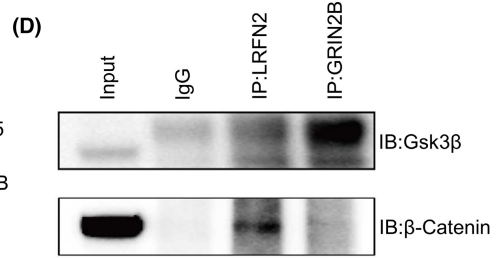
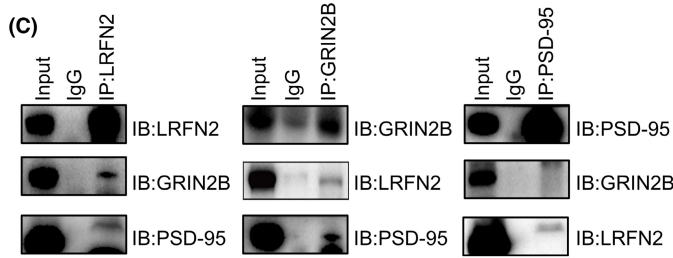
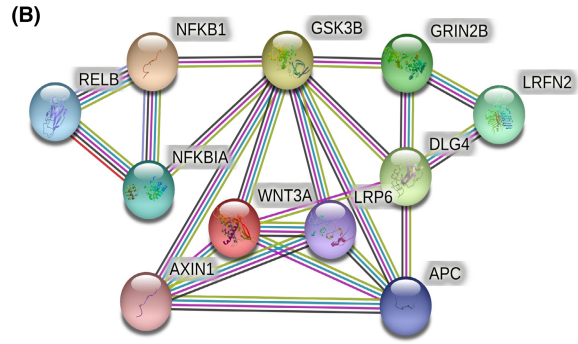
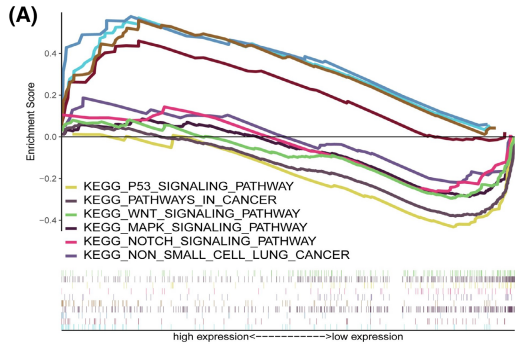
To observe the anti-ESCC effect of LRFN2, NOD/SCID mouse xenograft model of ESCC was established by subcutaneously injection with KYSE30 cells and LRFN2 overexpression KYSE30 cells (Figures 3A and S3). The results showed that the growth rate of subcutaneous tumor formation with KYSE30 cells overexpressing LRFN2 was significantly lower than that of the control group (Figure 3B,C; $*p < 0.05$, $**p < 0.01$). To clarify the effect of LRFN2 on the histological morphology of transplanted tumor of esophageal cancer, the transplanted tumor tissue was made into wax blocks and sections were stained with H&E (Figure 3E). It was observed that the tumor tissues of both groups were squamous cell carcinomas. In the control group, enlarged nuclei, deep staining, increased mitosis, and obvious tissue atypia was observed in cancer cells, whereas the pLVX-LRFN2 group showed lighter staining, smaller nuclei, and less tissue atypia, indicating that LRFN2 can cause histomorphology changes in esophageal carcinoma. The expression of LRFN2 and Ki67 in the transplanted tumors was detected using immunohistochemistry, and the

expression of Ki67 was significantly decreased in the pLVX-LRFN2 group with LRFN2 overexpression (Figure 3D,F). The results further confirmed that the overexpression of LRFN2 inhibited the growth of ESCC cells in vivo.

3.4 | LRFN2 inhibits Wnt/ β -catenin signaling pathway and NF- κ B pathway in ESCC

Bioinformatics analysis was conducted to explore the potential mechanism of ESCC inhibition by LRFN2. The results showed that the Wnt/ β -catenin signaling pathway was one of the most enriched pathways (Figures 4A and S4). The STRING database was applied to predict the protein–protein interaction. The results showed that there was an interaction between LRFN2, PSD-95, and NMDA receptor 2B subunit (GRIN2B; Figure 4B). It can be seen from the STRING data that LRFN2 affects GSK3B through GRIN2B, and previous reports have demonstrated that GRIN2B is one of the most important molecules in nerve and tumor growth.^{10,16–20,21,22} Therefore, the binding of GRIN2B, PSD-95, and LRFN2 was first tested by immunoprecipitation, the result showed that GRIN2B is the predominant binding protein of LRFN2 (Figure 4C), and further examination found that GRIN2B binds GSK3 β and that LRFN2 binds β -catenin (Figure 4D). Immunofluorescence results showed that LRFN2, PSD-95, and GRIN2B were colocalized in the nuclei of ESCC cells (Figure 4E). To verify whether LRFN2 regulates the Wnt/ β -catenin pathway, key proteins including p-GSK3 β , β -catenin, c-Myc, and cyclin D1 in ESCC cells (TE1 and KYSE30) and xenograft tumors were detected. As shown in Figure 4F, p-GSK3 β (ser389) was upregulated, whereas β -catenin, c-Myc, and cyclin D1 were downregulated by LRFN2 overexpression, the opposite results were obtained in the interfering LRFN2 group. Immunohistochemical staining (Figure S5) for β -catenin, p-GSK3 β , c-Myc, and cyclin D1 in xenograft tumors showed consistent results. To determine whether LRFN2 regulated the NF- κ B pathway, we use western blotting to verify the expression of key proteins in the NF- κ B pathway. The expression of NF- κ B and BCL2 was inhibited when LRFN2 was overexpressed. After knocking down LRFN2, the expression of NF- κ B and BCL2 increased (Figure 4G). Then, we used RSPO-1 (MCE,

FIGURE 4 LRFN2 regulates the Wnt/ β -catenin pathway and the NF- κ B pathway. (A) The dataset for LRFN2 expression in ESCC from the Kyoto Encyclopedia of Genes and Genomes (KEGG) database was assessed using bioinformatics and gene set enrichment analysis (GSEA). The results showed that, among all enrichment pathways, LRFN2 was most likely to regulate the Wnt/ β -catenin pathway. (B) Network prediction and annotation of LRFN2 with other molecules was performed using the STRING database. (C) Co-immunoprecipitation experiments revealed that LRFN2, GRIN2B, and PSD-95 bind to each other. (D) Using immunoprecipitation, we found that GRIN2B binds to GSK3 β and LRFN2 binds to β -catenin. (E) Immunofluorescence experiments showed that LRFN2, GRIN2B, and PSD-95 were colocalized in the nucleus of esophageal squamous cell carcinoma cells. (F) LRFN2 overexpression upregulated the expression of p-GSK3 β and downregulated the expression levels of β -catenin, c-Myc, and cyclin D1 in TE1 and KYSE30 cells. In a xenograft tumor, LRFN2 inhibited the key proteins of the Wnt/ β -catenin pathway, which was consistent with the results of experiments in vitro. After knockdown of LRFN2 expression in KYSE150, the changes in key proteins in the WNT pathway were opposite to those when LRFN2 was overexpressed. (G) Expression of NF- κ B and BCL2 was inhibited when LRFN2 was overexpressed. However, after knocking down LRFN2, the expression of NF- κ B and BCL2 increased. (H) Using RSPO-1 to agonize the WNT pathway, in the control group, the expression of β -catenin also increased with the increase in drug concentration. But in the LRFN2 overexpression group, β -catenin expression did not change with the increase in drug concentration. $*p < 0.05$, $**p < 0.001$



China) to characterize the Wnt/ β -catenin pathway, the expression of β -catenin also increased with the increase in drug concentration in the control group. But in the LRFN2 overexpression group, β -catenin expression did not change with the increase in drug concentration (Figure 4H). These results indicated that LRFN2 plays an inhibitory role in ESCC by regulating the Wnt/ β -catenin pathway and the NF- κ B pathway.

3.5 | LRFN2 binding to NMDAR affects the Wnt/ β -catenin pathway and NF- κ B pathway to inhibit the malignant phenotype of ESCC

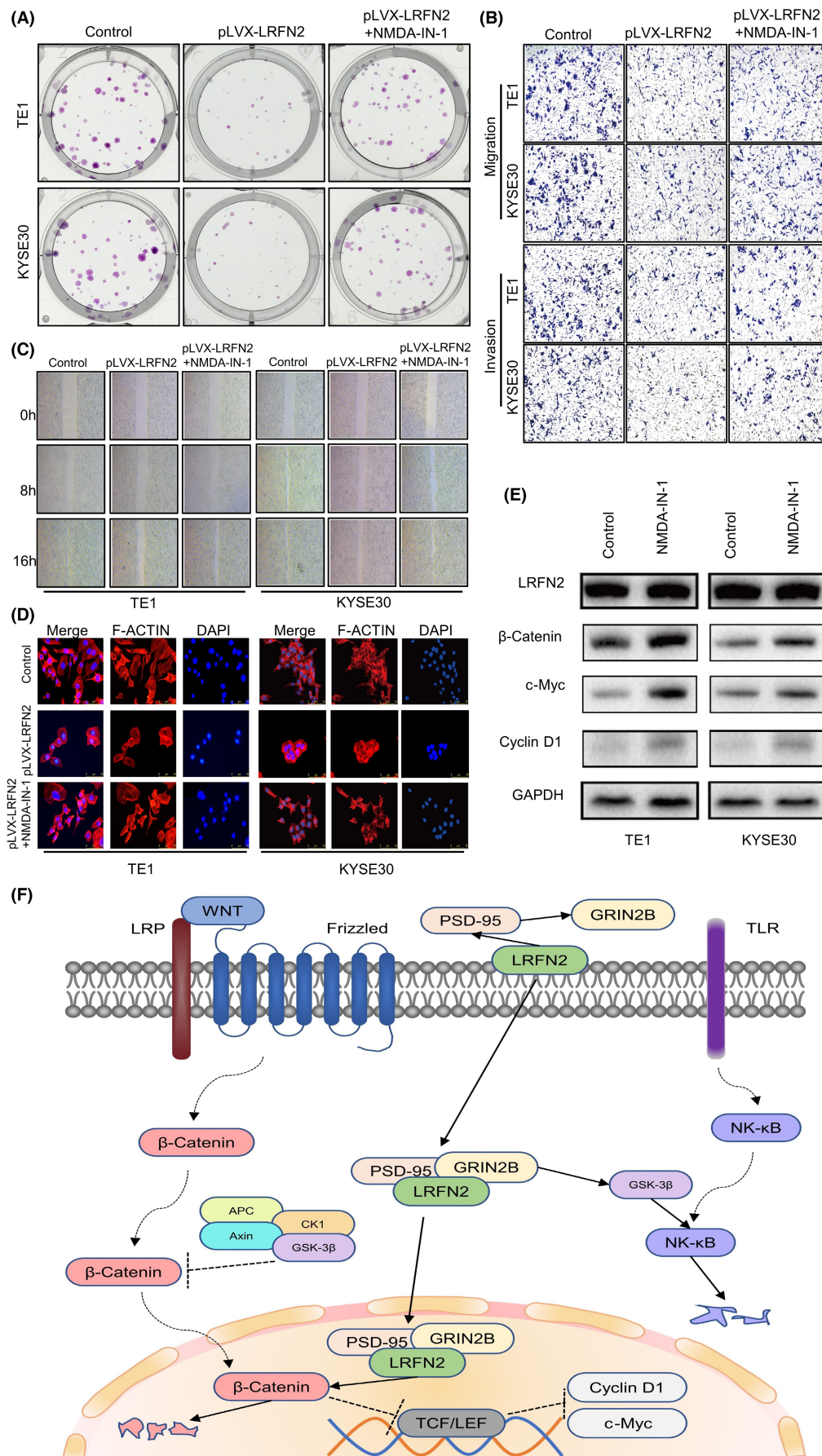
To verify whether LRFN2 plays an ESCC suppression role by binding with GRIN2B and regulate the Wnt/ β -catenin pathway and the NF- κ B pathway, ESCC cells were treated with GRIN2B-specific antagonist NMDA-IN-1 (MCE, China). Cell studies confirmed that proliferation (Figure 5A), migration, and invasion (Figure 5B) were inhibited by LRFN2 overexpression, the inhibitory effects could be reversed by NMDA-IN-1. Cell motility was detected by scratch assay, the results showed that the wound healing rate of NMDA-IN-1-treated cells was higher than that in the pLVX-LRFN2 group, indicating that LRFN2 inhibits the motility of ESCC cells through GRIN2B (Figure 5C). The effects of LRFN2 on actin F-actin through GRIN2B were detected by cellular immunofluorescence assay. Compared with the control group, the F-actin pseudopodia in the LRFN2 overexpression group decreased, indicating that the cell activity decreased at this time. When NMDA-IN-1 was added, the cells formed distinct pseudopodia, indicating that cell activity had increased compared with the previous state (Figure 5D). Data from Figure 5E showed that β -catenin, c-Myc, and cyclin D1 were up-regulated after NMDA-IN-1 treatment, indicating that the inhibition of GRIN2B can block the regulatory effect of LRFN2 on the ESCC. Collectively, LRFN2 recruits GRIN2B through PSD-95 on the cell membrane to form a complex and then enters the cell. In the cytoplasm, GRIN2B interacts with NF- κ B to block the NF- κ B pathway. In the nucleus, LRFN2 interacts with β -catenin to block the WNT pathway (Figure 5F).

4 | DISCUSSION

LRFN2, a member of the synaptic adhesion-like molecules family, has been reported to interact with NMDAR to disrupt hematopoietic differentiation and increase erythropoiesis, and cooperate with Myc to cause erythroblastosis.²³ LRFN2 organizes synapse development by promoting F-actin/phosphatidylinositol 4,5-bisphosphate-dependent clustering of neuroligin.²⁴ However, few studies have examined the mechanism of LRFN2 in tumors. As the first class of glutamate receptors and major excitatory neurotransmitter receptors, NMDAR family members are endogenously expressed neurotoxic molecules that can be activated in a variety of normal neurophysiological processes.¹⁴ They are thought to be critical to the physiological processes in the mammalian central nervous system and play a key role in spatial learning and memory.⁸ Some NMDAR subunits have been detected in nonneural tissues, for instance NMDARs are expressed in suprabasal keratinocytes and inhibit keratinocyte outgrowth necessary for some epithelialization processes.²¹ Notably, NMDAR2B is methylated at a high frequency in primary ESCC and has strong apoptotic activity in ESCC cell lines.^{18,19} NMDAR2B methylation in the promoter was shown to be an independent prognostic marker of ESCC survival,¹⁹ and the same results were observed in gastric cancer.²² Although these studies demonstrated the involvement of NMDAR in the development of tumors, the dysregulation and potential mechanisms of the LRFN2/NMDAR complex in ESCC progression remain largely unknown.

In this study, we found that the LRFN2/NMDAR complex directly interacts with and activates GSK3 β , which plays a tumor suppressor role by inhibiting cell metastasis mediated by the Wnt/ β -catenin pathway. In previous studies of the WNT pathway,²⁵⁻³² it is generally believed that GSK3 β can promote the ubiquitination and degradation of β -catenin when the WNT pathway is closed. The function of GSK3 β is related to its phosphorylation site. Studies have shown that the expression of p-GSK3 β (SER9) is downregulated when the WNT pathway is closed, and that the downregulation of β -catenin is a concomitant relationship rather than a causal relationship.³³ In the present study,^{30,31,32,34,35,36} we found that p-GSK3 β (SER389) is elevated when the WNT pathway is turned off, which is paradoxical

FIGURE 5 LRFN2 affects the Wnt/ β -catenin pathway and NF- κ B pathway through NMDAR to inhibit the malignant phenotype of ESCC. (A) The NMDAR antagonist's effects on the TE1 and KYSE30 proliferation. Through the plate cloning experiment, the inhibitory effect of LRFN2 on ESCC cell growth was weakened and the number of colonies increased compared with the pLVX-LRFN2 group. (B) Effect of the NMDAR antagonist on the TE1 and KYSE30 migration and invasion. The results showed that NMDA-IN-1 could promote the invasion and migration of ESCC cells in pLVX-LRFN2 cells. (C) The scratch healing rate increased significantly in NMDA-IN-1-treated pLVX-LRFN2 cells. The results displayed that the scratch healing rate increased significantly in pLVX-LRFN2 cells after treatment with NMDA-IN-1. (D) F-actin fluorescence intensity of the control, pLVX-LRFN2, and NMDA-IN-1-treated groups. The F-actin morphology of the overexpression group was rounder compared with the control group, indicating that cell activity decreased at this time. When NMDA-IN-1 was added, F-actin extended its tentacles, indicating that cell activity increased compared with the previous state. (E) After adding NMDA-IN-1, the expression levels of β -catenin, c-Myc, and cyclin D1 were higher compared with the control group. (F) LRFN2 recruits GRIN2B through PSD-95 on the cell membrane to form a complex and then enters the cell. In the cytoplasm, GRIN2B interacts with NF- κ B to block the NF- κ B pathway. In the nucleus, LRFN2 interacts with β -catenin to block the WNT pathway. * $p < 0.05$, ** $p < 0.01$.



with previous studies. In previous studies, it is generally believed that *p*-GSK3 β (SER389), like *p*-GSK3 β (SER9), is decreased when the WNT pathway is closed, whereas GSK3 β (TYR216)²⁷ is increased, promoting the phosphorylation of β -catenin and the final ubiquitination degradation. We cannot determine whether the increase in *p*-GSK3 β (SER389) has also a concomitant relationship with the decrease in β -catenin found in this study, and further study on the function of *p*-GSK3 β (SER389) is needed to clarify this question.

In the STRING data, LRFN2 affects GSK3 β through GRIN2B, thereby affecting the WNT pathway and the NF- κ B pathway, the expression of NF- κ B and BCL2 was inhibited when LRFN2 was overexpressed. However, after knocking down LRFN2, the expression of NF- κ B and BCL2 increased. Studies have shown that GSK3B can stimulate the NF- κ B pathway,³⁷⁻³⁹ so we hypothesized whether LRFN2 could affect the NF- κ B pathway due to changes in *p*-GSK3B (SER389), thereby affecting the occurrence of ESCC. This means that LRFN2 affects both the WNT and NF- κ B signaling pathways through GRIN2B, and the key molecule is GSK3 β . GSK3 β plays different functions in these two pathways and the function of its phosphorylation site SER389 needs to be re-examined. The change in its expression may not be directly related to the degradation of β -catenin, which means that GSK3 β 's role is not as important as imagined in the WNT pathway.

Based on the present results, LRFN2 may not regulate β -catenin through GSK3 β and its phosphorylation site SER389. So why does the expression of β -catenin also change no matter whether LRFN2 is overexpressed or disturbed? According to the experimental results, LRFN2 aggregates in the nucleus, and immunoprecipitation shows that LRFN2 and β -catenin have a strong interaction, so the place where LRFN2 affects β -catenin may be in the nucleus, and the functional study of LRFN2 in the nucleus is of great value.

In conclusion, LRFN2, a tumor suppressor, is decreased in cancer tissues and plays a crucial role in the progression of ESCC. Our study illustrated for the first time that LRFN2 can bind to NMDAR to inhibit the Wnt/ β -catenin pathway and the NF- κ B pathway. Our results support the use of LRFN2 as a potential therapeutic target for inhibiting the development of esophageal cancer and as an independent prognostic marker useful for patient survival. However, the specific mechanism by which the LRFN2/NMDA complex affects ESCC requires further study.

AUTHOR CONTRIBUTIONS

Yu Zhou: contributed significantly to experiment, analysis, and manuscript writing. Lijuan Xu: performed the data analyses and wrote the manuscript. Jiru Wang, Beibei Ge, Qiuzi Wang, Tao Wang, Chang Liu, and Bin Wei: performed some experiments. Qilong Wang: helped perform the analysis with constructive discussion. Yong Gao: contributed to the conception of the study and provided financial and technical support.

ACKNOWLEDGMENTS

This research is sponsored by the Jiangsu Natural Science Foundation of China (grant no. BK20211112), the Jiangsu Natural Science

Foundation of China (grant no. BK20211111), and the Foundation of Nanjing Medical University (grant no. NMUB2020133). Funding agencies do not interfere in subject design, data collection and analysis, or manuscript writing.

DISCLOSURE

The authors have no conflict of interest.

ETHICS STATEMENT

- Approval of the research protocol by an Institutional Reviewer Board: This study was approved by the Ethical Committee of Huai'an No. 1 People's Hospital, Nanjing Medical University (YX-P-2020-065-01).
- Informed consent: Informed consent of all patients was obtained before the study was conducted.
- Registry and the registration no. of the study/trial: N/A.
- Animal studies: All experiments were approved by the Animal Care and Use Committee of The Affiliated Huaian No. 1 People's Hospital of Nanjing Medical University (DW-P-2018-007-01).

ORCID

Yu Zhou  <https://orcid.org/0000-0003-0457-221X>

Qilong Wang  <https://orcid.org/0000-0002-5116-9186>

Yong Gao  <https://orcid.org/0000-0002-9537-0228>

REFERENCES

1. Sung H, Ferlay J, Siegel RL, et al. Global cancer statistics 2020: GLOBOCAN estimates of incidence and mortality worldwide for 36 cancers in 185 countries. *CA Cancer J Clin.* 2021;71:209-249.
2. Hu X, Wu D, He X, et al. circGSK3 β promotes metastasis in esophageal squamous cell carcinoma by augmenting β -catenin signaling. *Mol Cancer.* 2019;18:160.
3. Xiong JX, Wang YS, Sheng J, et al. Epigenetic alterations of a novel antioxidant gene SLC22A3 predispose susceptible individuals to increased risk of esophageal cancer. *Int J Biol Sci.* 2018;14:1658-1668.
4. Pennathur A, Gibson MK, Jobe BA, Luketich JD. Oesophageal carcinoma. *Lancet.* 2013;381:400-412.
5. Lin DC, Wang MR, Koeffler HP. Genomic and epigenomic aberrations in esophageal squamous cell carcinoma and implications for patients. *Gastroenterology.* 2018;154:374-389.
6. Lin DC, Hao JJ, Nagata Y, et al. Genomic and molecular characterization of esophageal squamous cell carcinoma. *Nat Genet.* 2014;46:467-473.
7. Song Y, Li L, Ou Y, et al. Identification of genomic alterations in oesophageal squamous cell cancer. *Nature.* 2014;509:91-95.
8. Morimura N, Yasuda H, Yamaguchi K, et al. Autism-like behaviours and enhanced memory formation and synaptic plasticity in Lrfn2/SALM1-deficient mice. *Nat Commun.* 2017;8:15800.
9. Ko J, Kim S, Chung HS, et al. SALM synaptic cell adhesion-like molecules regulate the differentiation of excitatory synapses. *Neuron.* 2006;50:233-245.
10. Morimura N, Inoue T, Katayama K, Aruga J. Comparative analysis of structure, expression and PSD95-binding capacity of Lrfn, a novel family of neuronal transmembrane proteins. *Gene.* 2006;380:72-83.
11. Jin G, Ma H, Wu C, et al. Genetic variants at 6p21.1 and 7p15.3 are associated with risk of multiple cancers in Han Chinese. *Am J Hum Genet.* 2012;91:928-934.

12. Verma S, Bakshi D, Sharma V, et al. Genetic variants of DNAH11 and LRFN2 genes and their association with ovarian and breast cancer. *Int J Gynaecol Obstet*. 2020;148:118-122.
13. Wang J, Wang Q, Wei B, et al. Intronic polymorphisms in genes LRFN2 (rs2494938) and DNAH11 (rs2285947) are prognostic indicators of esophageal squamous cell carcinoma. *BMC Med Genet*. 2019;20:72.
14. Boehning D, Snyder SH. Novel neural modulators. *Annu Rev Neurosci*. 2003;26:105-131.
15. Stepulak A, Rola R, Polberg K, Ikonomidou C. Glutamate and its receptors in cancer. *J Neural Transm (Vienna)*. 2014;121:933-944.
16. North WG, Gao G, Memoli VA, Pang RH, Lynch L. Breast cancer expresses functional NMDA receptors. *Breast Cancer Res Treat*. 2010;122:307-314.
17. Choi SW, Park SY, Hong SP, Pai H, Choi JY, Kim SG. The expression of NMDA receptor 1 is associated with clinicopathological parameters and prognosis in the oral squamous cell carcinoma. *J Oral Pathol Med*. 2004;33:533-537.
18. Kim MS, Yamashita K, Baek JH, et al. N-methyl-D-aspartate receptor type 2B is epigenetically inactivated and exhibits tumor-suppressive activity in human esophageal cancer. *Cancer Res*. 2006;66:3409-3418.
19. Kim MS, Yamashita K, Chae YK, et al. A promoter methylation pattern in the N-methyl-D-aspartate receptor 2B gene predicts poor prognosis in esophageal squamous cell carcinoma. *Clin Cancer Res*. 2007;13:6658-6665.
20. Wang CY, Chang K, Petralia RS, Wang YX, Seabold GK, Wenthold RJ. A novel family of adhesion-like molecules that interacts with the NMDA receptor. *J Neurosci*. 2006;26:2174-2183.
21. Nahm WK, Philpot BD, Adams MM, et al. Significance of N-methyl-D-aspartate (NMDA) receptor-mediated signaling in human keratinocytes. *J Cell Physiol*. 2004;200:309-317.
22. Liu JW, Kim MS, Nagpal J, et al. Quantitative hypermethylation of NMDAR2B in human gastric cancer. *Int J Cancer*. 2007;121:1994-2000.
23. Castellanos A, Lang G, Frampton J, Weston K. Regulation of erythropoiesis by the neuronal transmembrane protein Lrnf2. *Exp Hematol*. 2007;35:724-734.
24. Brouwer M, Farzana F, Koopmans F, et al. SALM1 Controls synapse development by promoting F-Actin/PIP2-dependent neurexin clustering. *EMBO J*. 2019;38:e101289.
25. Nusse R, Clevers H. Wnt/ β -catenin signaling, disease, and emerging therapeutic modalities. *Cell*. 2017;169:985-999.
26. Zhu L, Zhang X, Fu X, et al. TIPE2 suppresses progression and tumorigenesis of esophageal carcinoma via inhibition of the Wnt/ β -catenin pathway. *J Transl Med*. 2018;16:7.
27. Ye-Lim P, Hwang-Phill K, Young-Won C, et al. Activation of WNT/ β -catenin signaling results in resistance to a dual PI3K/mTOR inhibitor in colorectal cancer cells harboring PIK3CA mutations. *Int J Cancer*. 2018;144:389-401.
28. Duda P, Akula SM, Abrams SL, et al. Targeting GSK3 and associated signaling pathways involved in cancer. *Cell*. 2020;9:1110.
29. Papadopoli D, Pollak M, Topisirovic I. The role of GSK3 in metabolic pathway perturbations in cancer. *Biochim Biophys Acta Mol Cell Res*. 2021;1868:119059.
30. Zheng YW, Li ZH, Lei L, et al. FAM83A promotes lung cancer progression by regulating the Wnt and hippo signaling pathways and indicates poor prognosis. *Front Oncol*. 2020;10:180.
31. Chen Y, Li Y, Wang XQ, et al. Phenethyl isothiocyanate inhibits colorectal cancer stem cells by suppressing Wnt/ β -catenin pathway. *Phytother Res*. 2018;32:2447-2455.
32. Conti A, Majorini MT, Fontanella E, et al. Lemur tyrosine kinase 2 (LMTK2) is a determinant of cell sensitivity to apoptosis by regulating the levels of the BCL2 family members. *Cancer Lett*. 2017;389:59-69.
33. Beurel E, Grieco SF, Jope RS. Glycogen synthase kinase-3 (GSK3): regulation, actions, and diseases. *Pharmacol Ther*. 2015;148:114-131.
34. Cheng X, Qin L, Deng L, et al. SNX-2112 induces apoptosis and inhibits proliferation, invasion, and migration of non-small cell lung cancer by downregulating epithelial-mesenchymal transition via the Wnt/ β -catenin signaling pathway. *J Cancer*. 2021;12:5825-5837.
35. Wang Z, Yan H, Cheng D, et al. Novel lncRNA LINC01614 facilitates bladder cancer proliferation, migration and invasion through the miR-217/RUNX2/Wnt/ β -catenin Axis. *Cancer Manag Res*. 2021;13:8387-8397.
36. Liu Y, Li W, Luo J, et al. Cysteine-rich intestinal protein 1 served as an epithelial ovarian cancer marker via promoting Wnt/ β -catenin-mediated EMT and tumour metastasis. *Dis Markers*. 2021;2021:3566749.
37. Fu X, Zhong X, Chen X, Yang D, Zhou Z, Liu Y. GSK-3 β activates NF- κ B to aggravate caerulein-induced early acute pancreatitis in mice. *Ann Transl Med*. 2021;9:1695.
38. Oeckinghaus A, Hayden MS, Ghosh S. Crosstalk in NF- κ B signaling pathways. *Nat Immunol*. 2011;12:695-708.
39. Khan MS, Halagowder D, Devaraj SN. Methylated chrysin induces co-ordinated attenuation of the canonical Wnt and NF- κ B signaling pathway and upregulates apoptotic gene expression in the early hepatocarcinogenesis rat model. *Chem Biol Interact*. 2011;193:12-21.

SUPPORTING INFORMATION

Additional supporting information can be found online in the Supporting Information section at the end of this article.

How to cite this article: Zhou Y, Xu L, Wang J, et al. LRFN2 binding to NMDAR inhibits the progress of ESCC via regulating the Wnt/ β -Catenin and NF- κ B signaling pathway. *Cancer Sci*. 2022;113:3566-3578. doi: [10.1111/cas.15510](https://doi.org/10.1111/cas.15510)